

## Accurate Charge Density—Pendellosung Methods\*

*Norio Kato*

Department of Physics, Meijo University,  
Tempaku-ku, Nagoya, Japan.

### *Abstract*

We review various Pendellösung methods for the determination of crystal structure factors. Historical matters and the methodological principles are emphasised. We also describe the current state for the case of Si. Some deformation maps based on our recent experiment (Saka and Kato 1986) are presented. It is pointed out that the real part of the anomalous dispersion term has to be determined more accurately.

### 1. Introduction

The accurate determination of the charge density in solids through X-ray diffraction is one of main branches of modern crystallography. The possibility was recognised a long time ago for the simple reason that X-rays are scattered by electrons. Nevertheless, until sufficient knowledge was accumulated about diffraction physics, the nature of real crystals and computational techniques etc., one could not expect meaningful results. For this reason, it is only recently that this field has begun to contribute significantly to solid state physics and chemistry. Since the electronic structure is the basis on which one can understand the physico-chemical properties of matter, extensive research along this line is desirable.

It is natural to classify the approach into two categories according to the type of diffraction theory, kinematical or dynamical, with which one intends to obtain the accurate value of the crystal structure factor  $F_g$ . They will be denoted by K and D, respectively, in this paper.

The K approach is widely applicable to any type of crystal. In particular, since strong X-ray sources have become available, one can expect that more complex crystals, and those under some extreme conditions and even surface structures, will be investigated in near future. The attainable accuracy or reliability of  $F_g$  values has been much improved recently by overcoming intrinsic difficulties such as extinction and diffuse scattering.

Nevertheless, it seems that a high accuracy at the 0.1% level is attainable only by using the D approach, particularly the Pendellösung method, in the case of Si. For this reason, remembering also the importance to semiconductor physics, the results of Si are worth taking up as a case study for investigating the solid state effects of

\* Paper presented at the International Symposium on Accuracy in Structure Factor Measurement, held at Warburton, Australia, 23-26 August 1987.

the charge distribution. In Sections 2–4, the Pendellösung method is reviewed within the scope of diffraction physics. Following this review, in Section 5, the present state of the art on Si is presented with some new materials regarding the interpretation of our recent work (Saka and Kato 1986).

## 2. Pendellösung Methods: Introductory Remarks

The Pendellösung oscillation of the X-ray intensity field in perfect crystals was predicted by Ewald (1916, 1917). Fig. 1 reproduces an illustration in his extensive review article (Ewald 1933). The essence of the dynamical diffraction is that a plane wave outside the crystal creates two kinds of Bloch wave (two-wave approximation), which make a sinusoidal interference field. The theory of this type is called plane wave theory.

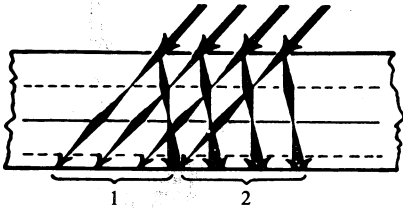


Fig. 1. Pendellösung fringes in perfect crystals expected in the plane wave theory. [From Ewald (1933).]

The phenomenon, however, could not be experimentally detected until 1959 by Kato and Lang. The main reason for this was that sufficiently large and perfect crystals had not been easily obtained. Fortunately, technological demands for Si perfect crystals advanced crystal growth techniques considerably, so that the principal obstacle was eliminated. Another significant element of this success was transmission topography introduced by A. R. Lang. By means of this technique, the X-ray intensity field could be observed with a resolution better than a few  $\mu\text{m}$ .

Since then, the dynamical diffraction phenomena or the X-ray optics have been extensively studied. These works together with the earlier achievements, notably the Laue (1931) theory and Borrmann's (1941, 1950) discovery of anomalous transmission, have elucidated the details of dynamical phenomena. The developments in this period has been reviewed, for example, by Batterman and Cole (1964) and by Kato (1974).

The Pendellösung method may be classified into three categories according to the experimental techniques and the theoretical formulae employed:

- (1) the section topography—the spherical wave theory;
- (2) the rocking curve measurement—the plane wave theory; and
- (3) the integrated intensity.

Before going into these subjects, the plane wave and spherical wave theories will be briefly explained.

The section topograph is obtainable by the simpler set-up of diffraction experiments with the use of characteristic X-rays. Fig. 2 is a schematic diagram showing the underlying principle. Inside the crystal one can expect a set of hyperbolic surfaces of equal intensity. With the use of an edge-shaped crystal, therefore, we will have a set of interference fringes on the exit surface which also have a hyperbolic form. The projection of this onto the photographic plate is called the section topograph. The topograph appears differently from what is expected from Fig. 1. Under the same conditions as Fig. 2 the fringes would be parallel to the top edge of the wedge.

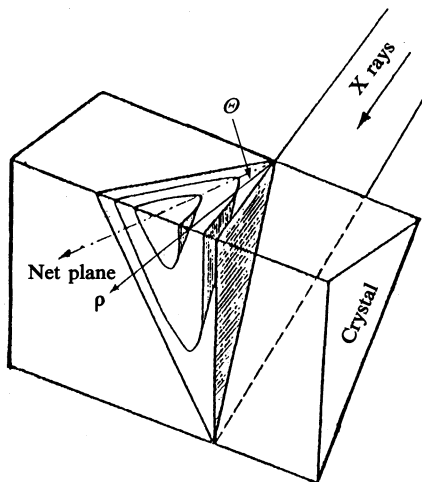


Fig. 2. Principle of section topography:  $\rho$  is an arbitrary direction in the reflection plane, namely the upper rectangular plane, and  $\theta$  is the angle between the  $\rho$  direction and the net plane.

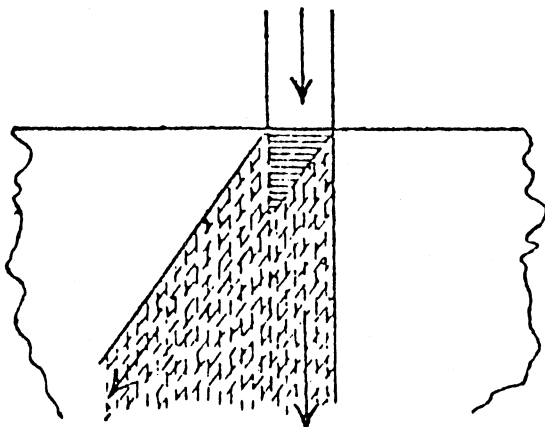


Fig. 3. General case of the incident wave. [From Ewald (1917).]

The difference indicates the necessity to develop a somewhat different theory from the original Ewald theory. This does not mean, however, any fundamental alteration in its theoretical framework. All one needs is to take a spherical wave, instead of a plane wave, as the incident wave, which is known as the spherical wave theory. Ewald (1917) already clearly recognised this situation as shown in Fig. 3. In this context he stated: 'The (plane wave) theory can be applied only to the (horizontally) hatched region where the incident and diffracted waves overlap completely. The experimentally available incident wave must be a superposition of plane waves, which have mutually definite phase relations.' Unknowingly, the present author used this idea extensively in developing his spherical wave theory. In fact, the spherical wave solution is obtained by superimposing the plane wave solution with a fixed phase relation.

It is interesting to consider the situation in terms of the bra and ket notation. The plane wave  $A_p | k_e \rangle$  having the wave vector  $k_e$  and the amplitude  $A_p$  is represented by the wavefunction  $A_p \langle r | k_e \rangle = A_p \exp\{i(k_e \cdot r)\}$  in  $r$ -space, and also  $A_p \langle k | k_e \rangle = A_p \delta(k - k_e)$  in  $k$ -space. As far as the diffraction phenomenon is concerned, the spherical wave is well approximated by  $A_s | r_e \rangle$ , where  $r_e$  is the entrance point and  $A_s$  is the amplitude depending on the source position. The wavefunction, therefore, has

the form  $A_s \langle r | r_e \rangle = A_s \delta(r - r_e)$  in  $r$ -space and  $A_s \langle k | r_e \rangle = A_s \exp\{-i(k \cdot r_e)\}$  in  $k$ -space. From this analysis, it is clear that the plane wave and spherical wave theories are complementary to each other in a wave-mechanical sense.

### 3. Basic Principles of Pendellösung Methods

Now we shall proceed to the basic principles of determining the structure factor  $F_g$ . For simplicity, only non-absorbing crystals are considered. Also, the symmetrical Laue case and a single mode ( $\pi$  or  $\sigma$ ) of polarisation are assumed for the incident wave, unless otherwise stated.

#### (a) Method of Section Topographs

According to the spherical wave theory (Kato 1960, 1961), the intensity field along the  $\rho$ -direction in Fig. 2 (specified by the angle  $\Theta$ ) is given by

$$I_s(\rho, \Theta) = |(A/\Lambda)J_0(\pi\rho/\Lambda_s)|^2, \quad (1)$$

where  $A$  is a constant,  $J_0$  is the Bessel function of zeroth order and  $\Lambda_s$ , which in fact is the asymptotic fringe spacing in the region of large  $\rho$ , is given by

$$\Lambda_s^{-1} = \cos\theta(1-p^2)^{\frac{1}{2}}\Lambda^{-1}, \quad (2a)$$

with

$$\Lambda = (mc^2/e^2)(\pi v/\lambda)(\cos\theta_B/C)(F_g F_{-g})^{-\frac{1}{2}}. \quad (2b)$$

In these equations

$$p = \tan\theta_B, \quad (3)$$

$v$  is the volume of the unit cell,  $C$  is the polarisation factor [ $1$ :  $\pi$ -mode;  $\cos 2\theta_B$ :  $\sigma$ -mode] and the other notation is standard. In the case of centro-symmetric crystals such as Si,  $F_g F_{-g}$  can be replaced by  $|F_g|^2$ . Usually  $\Lambda$  is of the order of  $10 \mu\text{m}$ .

Although there are technical problems in practice, one can determine  $\rho_{\max}$  and/or  $\rho_{\min}$  which correspond to maxima (minima) of the oscillatory intensity  $I_s$  (usually  $\Theta = 0$ ). Identifying these values multiplied by the coefficient  $\pi/\Lambda_s$  to the corresponding argument of  $J_0$ , one can determine  $\Lambda_s$  experimentally. In favorable cases, 30~40 extremum positions can be used so that  $\Lambda_s$  is determined accurately. It is straightforward to calculate  $|F_g|$  through equations (2) in which no ambiguity arises in the relative scale.

A preliminary attempt was made in the early work of Kato and Lang (1959) on Si and quartz. The more accurate measurement was carried out by Hattori *et al.* (1965), later by Hattori and Kato (1966) for Si, and by Yasuami and Homma (unpublished) for quartz. These results were summarised in the review article by Kato (1969).

Finally, it should be mentioned that a careful experiment with this method was reported by Tanemura and Kato (1972) and by Aldred and Hart (1973*a*, 1973*b*). In the latter work,  $|F_g|$  of 15 net planes were measured both at room and liquid nitrogen temperatures.

#### (b) Method of Rocking Curves

The rocking curve or the angular profile of the Bragg reflection is familiar to diffractionists. It is not difficult to understand the connection between the angular

oscillation of the profile and the topographic behaviour illustrated in Fig. 1. Since the fringe spacing (cf. equations 5 and 6) is very sensitive to the deviation of the glancing angle  $\theta$  from the exact Bragg angle  $\theta_B$ , the intensity of the Bragg reflection also changes rapidly as  $\theta$  is changed.

According to the plane wave theory, the intensity field of the Bragg reflection is given in the form

$$I_g(\theta) = I_e(1+y^2)^{-1} \sin^2(\pi t_0/\Lambda_p), \quad (4)$$

where  $I_e$  is the intensity of the incident wave,  $t_0$  is the crystal thickness and  $\Lambda_p$  is defined by

$$\Lambda_p^{-1} = (1+y^2)^{\frac{1}{2}} \Lambda^{-1}, \quad (5)$$

and where  $\Lambda$  has already been defined by equation (2b). The angular parameter  $y$  is defined by

$$y = (\theta - \theta_B) \sin \theta_B (\Lambda/\lambda). \quad (6)$$

An example of  $I_g(\theta)$  is given in Fig. 4. It should be noted that  $I_g(0)$  is not necessarily the peak value.

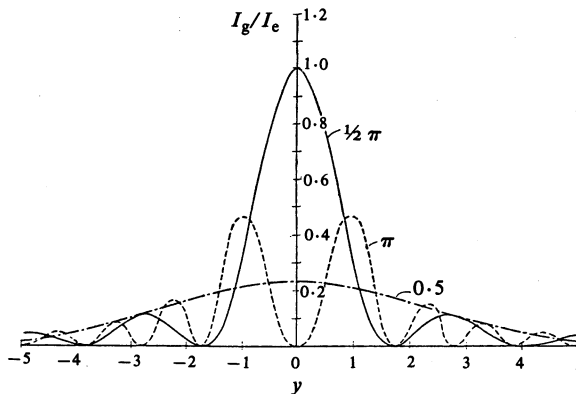


Fig. 4. Rocking curve in the Laue case (after Zachariasen 1945), where the three curves correspond to  $\pi t_0/\Lambda = \frac{1}{2}\pi$ ,  $\pi$  and  $0.5$ .

In practice, the angular period of the oscillation is of the order of  $0.1$  arcsec or less. For this reason, before about 1960, no one thought that the oscillation could be observed. Even the observation of the averaged profile, which must have a Lorentzian form (Ewald 1917) [letting  $\sin^2(\pi t_0/\Lambda_p) = \frac{1}{2}$  in equation (4)] with a halfwidth of a few arcsec, was a technically difficult matter for those days. At present, a novel method to make a monochromator and the specimen crystal from a monolithic crystal and techniques to measure one thousandth of a second enable us to carry out such sophisticated experiments (Deutsch and Hart 1985).

In principle, we can determine a set of the angular positions of the maxima (or minima) of the intensity  $I_g(\theta)$ , and calculate the corresponding  $y$ -values from equation (4). In the same way as in the case of method (1) we obtain  $\Lambda$ , and consequently  $|F_g|$ . Recently, Teworte and Bonse (1984) reported an accurate value of  $|F_g|$  for Si using this principle.

(c) Method of Integrated Intensity

The integrated intensity is also familiar to diffractionists. Conventionally, it is defined by the angular integration of (4) in the plane wave theory and denoted by  $R^\theta$ . From the standpoint of the spherical wave theory, it is the spatial integration of the intensity distribution (equation 1) over the exit surface. For the incident wave having the same angular and spatial characteristics, both procedures of integration give the same formula, as it should be so. The method using the traverse topographs, therefore, belongs to the category of concern here. At an early stage Batterman and Patel (1968) used this method for the measurement of a few  $|F_g|$  values of Ge.

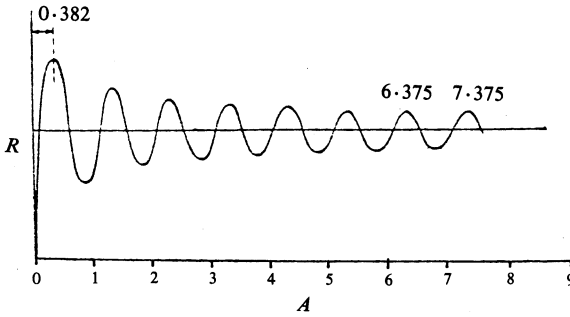


Fig. 5. Integrated intensity  $R = R^\lambda A(2d \cos \theta_B)$  against  $A = \pi t / \lambda$  (see equation 8).

For the accurate determination of charge density, in practice, it is convenient to deal with the integrated intensity using white radiation as mentioned below. Recalling Bragg's law, we get from equation (6)

$$dy \approx (\sin \theta_B)(A/\lambda) d\theta = (2d \cos \theta_B)^{-1}(\sin \theta_B)(A/\lambda) d\lambda, \quad (7)$$

for the narrow angular range corresponding to the rocking curve, where  $R^\lambda$  differs from  $R^\theta$  only by the factor  $2d \cos \theta_B$ . Thus, it turns out that the expression for  $R^\lambda$  is given by (apart from an irrelevant constant)

$$R^\lambda(t/A) = (d \cos \theta_B)^{-1}(1/A) \int_0^{2\pi t/A} J_0(q) dq, \quad (8)$$

where  $t$  is the effective thickness of the crystal and  $A$  is defined by equation (2b). The expression (8) has the behaviour shown in Fig. 5. Then, the oscillatory character can be used for determining  $A$  in the same manner as in the previous two methods. Here, one can conceive of two subcategories as practical methods:

(a) The method of  $\lambda$  variable: The parameter  $A$  includes the wavelength  $\lambda$ . Therefore, if one uses an incident beam having a reasonably narrow angular divergence from the X-ray source,  $R^\lambda$  can be considered principally as a function of  $\lambda$ . In practice, a  $\theta_B - 2\theta_B$  scanning of the crystal-counter system is used under the condition to record the Bragg-reflection beam. Care has to be taken as  $\theta_B$  also depends on  $\lambda$ . The method was first proposed by Takama *et al.* (1980).

(b) The method of  $t$  variable: If the crystal is rotated around the reflection vector  $g$ , with the incident beam similar to that in method (a), one can change the thickness  $t$  effectively according to the relation

$$t = t_0 / \cos \psi, \quad (9)$$

where  $\psi$  is the rotation angle from the vertical position and  $t_0$  is the thickness of the crystal. The idea was first introduced in Pendellösung phenomena by Utemisov *et al.* (1980), although it can be traced back much earlier in various diffraction experiments. If one uses the characteristic rays as the incident beam, keeping the exact Bragg condition during the  $\psi$  rotation is not easy unless high precision apparatus is employed. The difficulty is easily eliminated by the use of white radiation. Saka and Kato (1986) used this technique.

#### 4. Comments on Various Methods

It is impossible to state decisively which method is superior. The most important thing is how carefully the data are collected, and the necessary corrections which should be made for them. Nevertheless, a few obvious merits and demerits in each method can be pointed out here.

##### (a) Lattice Distortions

A long range lattice distortion is harmful in the Pendellösung method in general, just as is the extinction in the K approach. The lattice distortion is easily induced at every stage of sample preparation and in setting to the diffractometer. In the case of section topography the effects of the fringe spacing and the intensity distribution have been thoroughly worked out in terms of the spherical wave theory (Kato 1963, 1964) and experimentally well investigated (Hart 1966). Therefore, a reliable correction can be made at least when the strain is spatially linear. On the other hand, an understanding of corrections still remains qualitative in cases of the rocking curve and the integrated intensity.

Under the circumstances, it is desirable to find an experimental check point, for example, the asymmetric behaviour in the  $\pm\psi$  regions in method (3b). The same is true in methods (2) and (3a), in which the profiles of the  $\pm\theta$  and  $\pm\theta_B$  regions respectively have to be symmetric.

From the viewpoint of crystal growth, it is a great advantage if a large crystal is not required. Also, as far as sample preparation, it is a considerable advantage if parallel-sided crystals can be used. In these respects, the method of topography (1) seems less advantageous compared with others in which a small circular beam can be used. In any case, however, if a highly accurate measurement is attempted, the total specimen must be free from defects.

##### (b) Higher Order Reflections

In order to obtain an accurate charge density, it is desirable to measure the  $|F_g|$  of higher order reflections, as many as possible. From this viewpoint, method (1) is the most advantageous and method (2) is disadvantageous, because the fringe spacing is increased in method (1) whereas the angular width of the rocking curve itself is decreased in method (2) for smaller structure factors (cf. equations 2b and 6).

The integrated intensity method (3) has an intrinsic disadvantage because the oscillation is an averaged result of sinusoidal fringes having different spacing. According to our experiences, 880 is nearly the maximum order for the oscillation to be clearly observed. Now, the highest datum goes up to the (12, 12, 0) reflection in method (2) (Deutsch and Hart 1985).

Here we suggest the strategy of using the Pendellösung method up to a certain order, say 880, and then the K approach for the higher order reflections, because the strain criterion is more stringent in the former whereas the extinction is less harmful in the latter for higher order reflections.

### (c) Intensity Profile

So far the principle was explained in the simplest case as mentioned at the beginning of Section 3. The limited argument, of course, must be generalised to meet real experiments. The required theoretical formulae are available in several extensive reviews (see e.g. Kato 1974; Pinsker 1978). Then, we must confirm also how far the dynamical theory can describe the observed intensity profile.

Conclusively, the formulae derived from the dynamical theory agree fairly well with the experimental profile, provided that a term due to diffuse scattering is added. This situation is unavoidable because the conventional dynamical theory is concerned with only the coherent part, which is the Bragg reflection. Physically, there exist also the partially coherent and incoherent parts owing to the thermal vibration and some point-like defects. The problem has to be dealt with on the basis of a statistical treatment of optics. The statistical dynamical theory (Kato 1980) was a trial attempt along this line.

Here, we shall consider the effect from experimental viewpoints in the method (1) and (3b) based on our own experiences. With increasing the crystal thickness over the extinction distance ( $\sim \Lambda$ ), the dynamical formula tends to a constant ( $\sim 1/\Lambda$ ) independently of the crystal thickness  $t$ , as illustrated in Fig. 5. On the other hand, the incoherent part, which may be treated by the kinematical theory, increases proportionally with  $t$ . It is practically negligible for low order reflections (Wada and Kato 1977), but amounts to the same order of magnitude as the dynamical part for higher orders (Saka and Kato 1986). For a high precision measurement, therefore, the kinematical term must be taken into account. Fortunately, the term increases monotonically and gradually with increasing  $t$ . Moreover, the shifts of maximum and minimum positions are not only small but opposite, so that the net effect is quite small if one uses equal numbers of maxima and minima. In fact, this situation is a great advantage in the Pendellösung method compared with the K approach where the separation of the Bragg reflection and the diffuse scattering is cumbersome.

## 5. Current State of Si

### (a) Measurement of Structure Factor

In our recent work (SK), the  $|F_g|$  were measured with method (3b) for 30 net planes of Si. Prior to this, one-half had been measured by Aldred and Hart (AH, 1973a) and Teworte and Bonse (TB, 1984) with methods (1) and (2) respectively. Also,  $|F_g|$  of several net planes were measured by Tanemura and Kato (1972) and by Takama *et al.* (1980) in which methods (1) and (3a) were used respectively. This situation is extremely valuable in the task of accurate measurement. The validity

of methodology and the accuracy in the reported  $|F_g|$  values can be evaluated independently of any theoretical prejudice. One may claim that  $|F_g|$  values based on the Pendellösung method are at the 0.1% level and even better in several low-order reflections. The details are described in the SK (1986) paper.

It is worth mentioning that attempts have been made by the Takama–Sato group to extend the measurement to other materials such as GaAs, diamond, Zn etc. The values may be less accurate because sample crystals are not perfect as with Si.

### (b) Anomalous Dispersion Term

In order to obtain the structure factor intrinsic to the charge density, one must subtract from the observed value  $f_{ob}$  the correction term

$$\Delta f = (f' + f_{NT})e^{-M} \quad (10)$$

on the scale per atom, where  $f'$  is the real part of the anomalous dispersion and  $f_{NT} = 0.0038$  is the term due to nuclear Thomson scattering, which should not be neglected for very accurate measurements (Tanemura and Kato 1972).

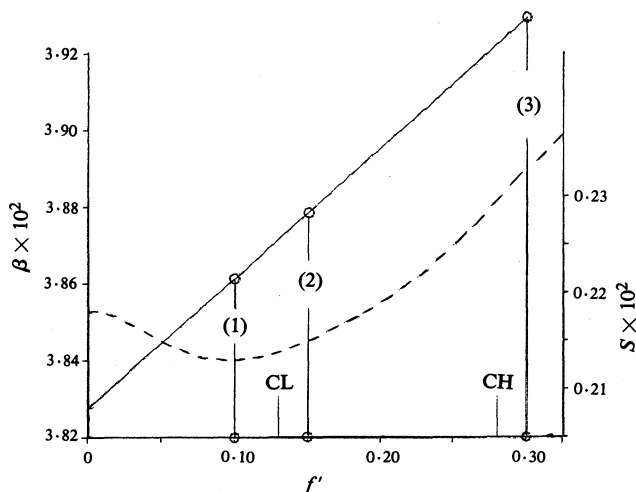


Fig. 6. Correlation of the temperature coefficient  $\beta$  and the anomalous dispersion term  $f'$ , where  $S$  is the relative standard deviation in the analysis (see Section 5b), CL is the Cromer–Lieberman (1970) value and CH is the Cusatis–Hart (1975) value.

Here, we come cross a subtle problem on the precise value of  $f'$ . Experimentally (Takeda and Kato 1978; Saka and Kato 1987) it has been confirmed that the  $\lambda$  dependence of  $f'$  over a range from 1.5 Å down to 0.3 Å agrees well with the theoretical prediction of Cromer and Liberman (CL, 1970), who dealt with anomalous dispersion due to photoelectric effects. Omote and Kato (OK, 1987) reformulated the theory with higher approximations\* and confirmed the validity. Also, this theory is free from the approximation of forward scattering. Unless the order of reflections is very high, let us say more than 880, the necessary corrections for CL values are less than 0.3%. According to the absolute measurement by Cusatis and Hart (1975),

\* CL calculated terms up to  $(v/c)^2$  whereas OK worked up to  $(v/c)^4$ , where  $v$  is the average velocity of electrons in atoms and  $c$  is the velocity of light.

however, the value is larger than the CL value by 0.015 for Si in the wavelength range of Ag and Mo  $K\alpha$ .

We have experimentally examined this discrepancy, though indirectly, based on Dawson's (1967*a*) theoretical conclusion that structure factors of even and higher order reflections must be normal; namely, no inharmonicity [ $M = \beta(h^2 + k^2 + l^2)$ ] and no bonding effect would be involved in them. The procedure of analysis is the following. First, we corrected our data set of even order higher than 642 with expression (10) by taking various  $f'$  covering CL and CH values, and then the Wilson plotting was applied to obtain the coefficient  $\beta$ . Fig. 6 shows  $\beta$  and the relative standard deviation  $S = \sigma/\beta$  against the assumed  $f'$ . Judging from the  $S$  minimum one can conclude that the CL value for  $f'$  fits well to the theoretical prediction.

For this reason, we used the CL values for the comparison among five data sets reported by AH, TB and SK. For the first two Mo and Ag  $K\alpha$  were used, whereas 0.4 Å white radiation was used by SK for collecting data. Our data were closer to the average value among the five data sets (SK 1980).

As a matter of fact, the  $\lambda$ -independent part of the ambiguity in  $f'$  is not harmful in this comparison. A serious problem, however, arises in the ambiguity of  $f'$  for obtaining the deformation charge. The subject will be discussed in the following subsection.

### (c) Deformation Charge

The deformation charge (DC) is simply the Fourier synthesis having the coefficients

$$\Delta_g = Q[f_{\text{ob}} - \Delta f - f_{\text{HF}} \exp\{-\beta(h^2 + k^2 + l^2)\}], \quad (11)$$

where  $\Delta f$  is the correction given by equation (10),  $f_{\text{HF}}$  is the Hartree–Fock scattering factor of an isolated atom (Clementi 1965) and  $Q$  is the crystal structure factor for a point atom of unit charge. Such a map helps us to visualise the solid state effect of the charge density. Since the aim of this article is to explain the principle of Pendellösung methods, only a few examples (see Fig. 7) are presented in order to show the quality of maps, which have an accuracy better than  $0.02 e \text{ \AA}^{-3}$ .

In constructing these maps, we need to amend the  $F_g$  values for forbidden reflections from other sources. Regarding the 222 reflection, Alkire *et al.* (1982) have proposed a value  $F_{222} = 1.456 \pm 0.008$ , obtained by the K approach in  $\gamma$ -ray diffraction. Here, however, we used the old value by Fehlman and Fujimoto (1975) of  $F_{222} = 1.645 \pm 0.030$  (at 293 K), in order to use the Pendellösung value in which method (1) was employed. Actually, no significant difference was recognised in final DC maps with the use of such slightly different values for a single net plane.

As mentioned above, the ambiguity in  $f'$  and  $\beta$  is rather serious. Any systematic error over all data in the Fourier coefficient  $\Delta_g$  often causes a different appearance of the DC. For examining this point in our particular case, we constructed DC maps for different sets of ( $f'$ ;  $\beta$ ), marked by the circles in Fig. 6. Fig. 8 shows the DC distributions along the 111 direction in several cases. Surprisingly, the distribution is insensitive to the choice of ( $f'$ ;  $\beta$ ) except near the atomic position. After this analysis, it is concluded that the bonding charge and the charge deficit in the anti-bonding region, illustrated in Fig. 7, must be reliable, but we urgently need to settle the problem in the  $f'$  value to obtain any conclusion on the deformation charge near the atomic position.

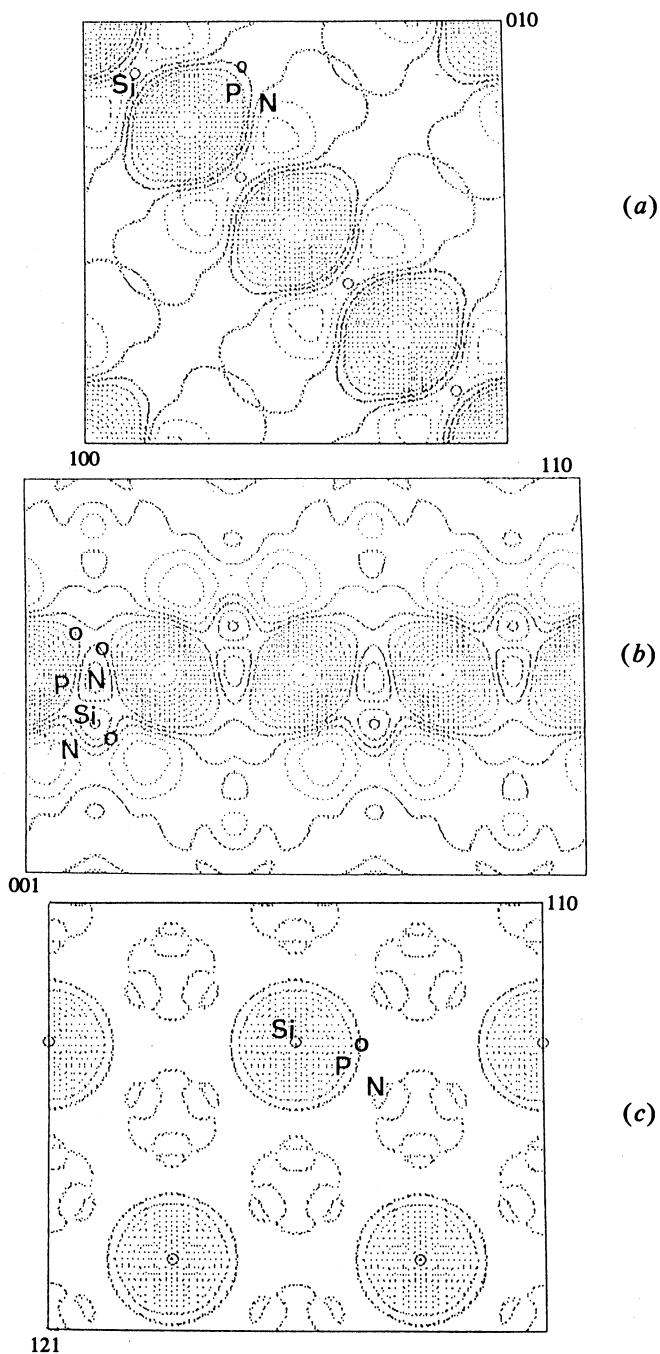


**Fig. 7.** Deformation charge maps based on the  $|F_g|$  data of SK (1986): (a) the 100 plane through the middle of bonding; (b) the 110 plane through Si atoms; and (c) the 111 plane through the middle of bonding. Shown are Si, the atomic position; o, the neutral contours; P, the positive region; and N, the negative region. The step unit of the contours is  $0.02 e \text{ \AA}^{-3}$ .

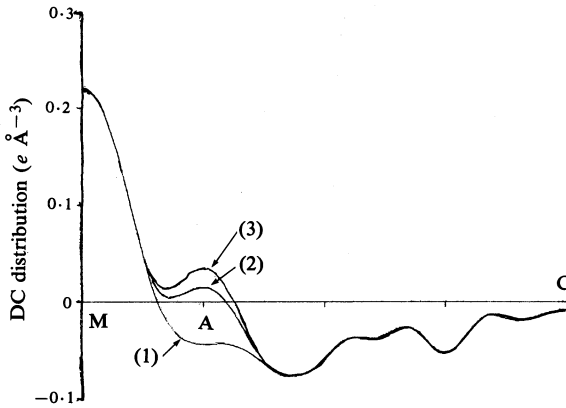


**Fig. 8.** DC distribution along the [111] direction for different choices of  $(f', \beta)$ . The curves (1), (2) and (3) correspond to three sets of the circled points in Fig. 6. The point M is the middle of the bonding, A is the atomic position, and C is the body centre of the unit cell.

#### (d) Comparison with Theoretical Charge Density

In order to complete our studies on solid state effects, it is important to compare the experiment with available theories. In the past, the number of reflections for which  $|F_g|$  values were measured was rather limited in the D approaches. Now we can compare not only  $|F_g|$  values but also the experimental DC map with the theoretical one in the manner common in many K approach studies.

In the case of diamond structures, Dawson (1967*b*, 1967*c*) extensively developed a theory to describe the charge density, and consequently the structure factor, in terms of a few phenomenological parameters. The theory is simply based on the site symmetry of atoms in the crystal using a pseudo-atomic model. He applied the theory to the data on C, Si and Ge available in those days. Later, in the case of Si, Aldred and Hart (1973*b*) and very recently Spackman (1986) analysed the measurements of AH (1973*a*) along this line with some modifications of the theory. The theory, however, has a limitation because the pseudo-atomic model is not quite sound for the covalent bond. Moreover, the theory is unsatisfactory in giving a true insight into the wavefunction.

On the other hand, the wavefunction in the solid state has been extensively investigated as an automatic by-product from energy band calculations. An attempt to compare existing theories of this sort with our recent experimental results has been presented by Cummings and Hart (1988, present issue p. 423). Partly for this reason and since much remains to be done for a reliable discussion, the author leaves this topic for the future.

## 6. Concluding Remarks

The Pendellösung method can determine  $F_g$  values not only accurately but also absolutely. Here, the present state of the art has been discussed for the case of Si. The author believes that the result is one of the significant achievements of the dynamical diffraction theory originated by Ewald. Also, it should be emphasised that accuracy

and reliability can be attained through the collective work of many scientists. Many technical matters, details of which could not be mentioned in this article, are vital to the future development in the cases of Si and other materials. Finally, the present author would like to express his thanks and appreciation to all colleagues.

## References

- Aldred, P. J. E., and Hart, M. (1973 *a*). *Proc. R. Soc. London A* **332**, 233.  
 Aldred, P. J. E., and Hart, M. (1973 *b*). *Proc. R. Soc. London A* **332**, 239.  
 Alkire, R. W., Yelon, W. B., and Schneider, J. R. (1982). *Phys. Rev. B* **26**, 3097.  
 Batterman, B. W., and Cole, H. (1964). *Rev. Mod. Phys.* **36**, 681.  
 Batterman, B. W., and Patel, J. R. (1986). *J. Appl. Phys.* **39**, 1882.  
 Borrmann, G. (1941). *Phys. Z.* **42**, 157.  
 Borrmann, G. (1950). *Z. Phys.* **127**, 297.  
 Clementi, E. (1965). 'Tables of Atomic Functions', Suppl. to *IBM J. Res. Dev.* **9**, 2.  
 Cromer, D. T., and Liberman, D. (1970). *J. Chem. Phys.* **55**, 1891.  
 Cummings, S., and Hart, M. A. (1988). *Aust. J. Phys.* **41**, 423.  
 Cusatis, C., and Hart, M. (1975). In 'Anomalous Scattering' (Eds S. Ramaseshan and S. C. Abrahams), p. 55 (Munksgaard: Copenhagen).  
 Dawson, B. (1967 *a*). *Proc. R. Soc. London A* **298**, 255.  
 Dawson, B. (1967 *b*). *Proc. R. Soc. London A* **298**, 264.  
 Dawson, B. (1967 *c*). *Proc. R. Soc. London A* **298**, 379.  
 Deutsch, M., and Hart, M. (1985). *Phys. Rev. B* **31**, 3846.  
 Ewald, P. P. (1916). *Ann. Phys. (Leipzig)* **49**, 117.  
 Ewald, P. P. (1917). *Ann. Phys. (Leipzig)* **54**, 519.  
 Ewald, P. P. (1933). In 'Handbuch der Physik', Bd XXIII/2 (Eds H. Geiger and K. Scheel), Ch. 4 (Springer: Berlin).  
 Fehlman, M., and Fujimoto, I. (1975). *J. Phys. Soc. Jpn* **38**, 208.  
 Hart, M. (1966). *Z. Phys.* **189**, 269.  
 Hattori, H., and Kato, N. (1966). *J. Phys. Soc. Jpn* **21**, 1772.  
 Hattori, H., Kuriyama, H., Katagawa, T., and Kato, N. (1965). *J. Phys. Soc. Jpn* **20**, 988.  
 Kato, N. (1960). *Z. Naturforsch.* **15a**, 369.  
 Kato, N. (1961). *Acta Cryst.* **14**, 526; 627.  
 Kato, N. (1963). *J. Phys. Soc. Jpn* **18**, 1785.  
 Kato, N. (1964). *J. Phys. Soc. Jpn* **19**, 67; 971.  
 Kato, N. (1969). *Acta Cryst.* **A 25**, 119.  
 Kato, N. (1974). In 'X-ray Diffraction' (Ed. L. Azaroff), Chs 4 and 5 (McGraw-Hill: New York).  
 Kato, N. (1980). *Acta Cryst.* **A 36**, 763; 770.  
 Kato, N., and Lang, A. R. (1959). *Acta Cryst.* **12**, 787.  
 Laue, M. von (1931). *Ergeb. Exakt Naturw.* **10**, 133.  
 Omote, K., and Kato, N. (1987). *Acta Cryst.* **A 43**, 255.  
 Pinsker, Z. G. (1978). 'Dynamical Scattering of X-rays in Crystals' (Springer: Berlin).  
 Saka, T., and Kato, N. (1986). *Acta Cryst.* **A 42**, 469.  
 Saka, T., and Kato, N. (1987). *Acta Cryst.* **A 43**, 252.  
 Spackman, M. A. (1986). *Acta Cryst.* **A 42**, 271.  
 Takama, T., Iwasaki, M., and Sato, S. (1980). *Acta Cryst.* **A 36**, 1025.  
 Takeda, T., and Kato, N. (1978). *Acta Cryst.* **A 34**, 43.  
 Tanemura, S., and Kato, N. (1972). *Acta Cryst.* **A 28**, 69.  
 Teworte, R., and Bonse, U. (1984). *Phys. Rev. B* **4**, 201.  
 Utemisov, K., Somenkova, V. P., Somenkov, V. A., and Shi'shtein, S. Sh. (1980). *Sov. Phys. Crystallogr.* **25**, 484.  
 Wada, M., and Kato, N. (1977). *Acta Cryst.* **A 33**, 161.  
 Zachariasen, W. H. (1945). 'Theory of X-ray Diffraction in Crystals' (Dover: New York).

